Richard H. Darling
Chen-Hsiung Lee
Lawrence Kuhn

# Multiple-Nozzle Ink Jet Printing Experiment

*An experimental printer is described which utilizes a densely packed array of ink jets operated in a binary, pressurized, asynchronous mode. The printer configuration, the ink jet head structure, the operating point, and the maintenance approach are all discussed.*

## Introduction

Nozzle-per-spot ink jet printing utilizes an array of nozzles (and associated charging electrodes) operated in a binary mode. Charged drops from each jet are deflected and intercepted by a common electrode and "drop catcher," whereas uncharged drops pass undisturbed to the paper. The binary mode obviates the need for sophisticated drop-placement algorithms and circuits required for analog ink jet print schemes [1]. These correction schemes become too complicated and costly when arrays of ink jet heads are required for high-throughput applications. The reduction of the burden on the electronic control is achieved by using more complicated structures. In fact, these structures are practical mainly because of developments in electronic semiconductor fabrication and packaging technology. Unlike previously described approaches, the nozzle-per-spot mode of printing described here is characterized by complete asynchronism between the drop formation process and the charging process. This is advantageous because of the relaxation of requirements on drop-formation characteristics, and is made possible because of the use of multiple drops per pel (picture element or spot). This paper focuses on the selection of the operating point for optimization of print quality, on the fabrication techniques, and on novel start-up and maintenance concepts. Underlying themes of the work are the use of planar batch fabrication techniques to minimize the incremental cost of adding more nozzles to the system and the choice of an operating point that minimizes sensitivity to structural nonuniformities rather than trying to get maximum printed throughput from each nozzle.

**Figure 1** shows one side of the print head, illustrating the basic binary ink jet configuration. There are a variety of possible printer configurations, which are strongly influenced by the print speed and paper path. For instance, for cut sheets, a useful approach is the extension of the classical facsimile geometry to an array of sources creating a set of interleaved helices on a rotating drum. Assuming that batch fabrication techniques are used, the jets could be packaged as close to each other as possible with the printing rate increased by extending the length of the array until it ultimately spanned the page. An alternative approach for high-speed printing is stationary, staggered arrays spanning the page. This is the approach pioneered by the Mead Corp. [2]. In general, two to four rows of nozzles are required because of the geometric factors associated with the charging electrode, which require an adjacent-jet distance of at least one pel. Printing rates as high as a thousand pages per minute are possible. Of course, the paper path in this case could be either cut sheet or continuous. In order to print at more modest rates (perhaps 50 to 100 pages per minute) on continuous paper (fanfold) as required for computer-output system printers, the configuration of **Figure 2** is most appropriate. The head is transported across the paper, filling in a complete band of image. The head prints in both directions and the paper is advanced during the head turnaround.

The latter approach has been the focus of this study. Some of the unique requirements associated with this approach are the small mass and size of the ink jet print head for ease of

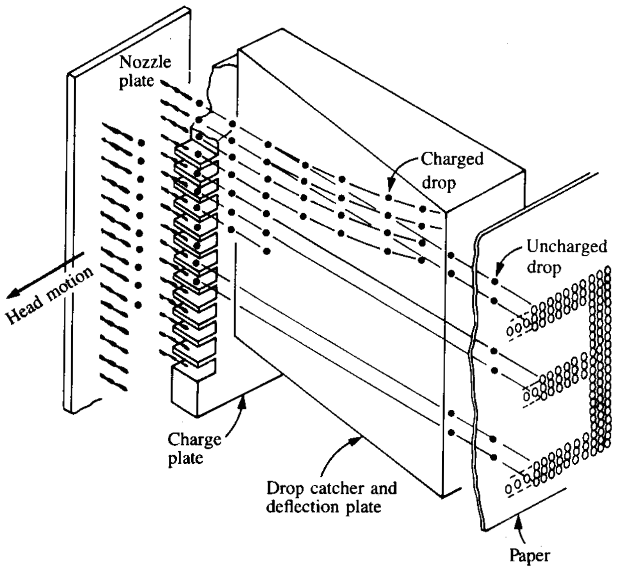


**Figure 1** Array of binary nozzles and the pattern formed by undeflected drops reaching the paper.

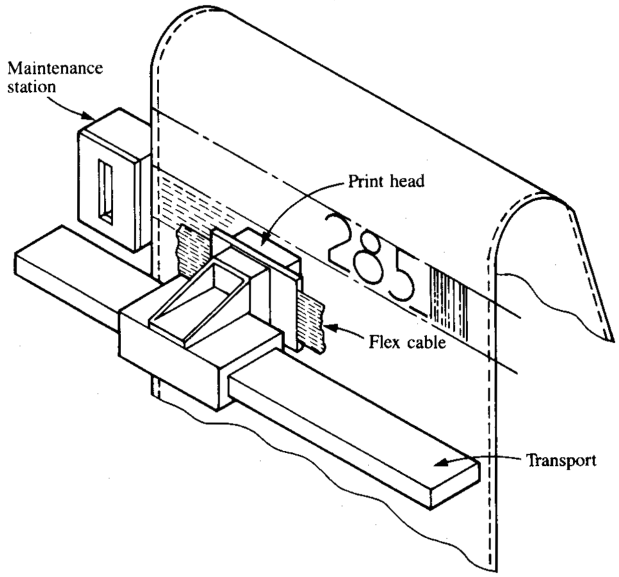


**Figure 2** Nozzle-per-spot printing configuration with head transported and continuous paper path.

transport; printing during acceleration to optimize throughput; low voltages to facilitate integration of drive electronics onto the moving head, thereby minimizing cabling complexity; and printing a fully filled band on each pass.

The transportability of the head makes it possible to put certain operations in a "maintenance station" off to one side of the paper. The maintenance station can perform a variety of functions, such as start-up aid, contamination cleansing, and drop-velocity sensing. These are discussed below.

## Printer system consideration

Some of the basic concepts of the nozzle-per-spot operating-point selection can be understood and verified experimentally by consideration of a single nozzle (**Figure 3**). The deflection of the individual drops can be approximated by

$$\Delta = \frac{4\varepsilon v_c}{d^2 \ell n(4s/\pi d)} \cdot \frac{V_d}{G} \cdot \frac{L^2}{v^2}, \qquad (1)$$

where $\varepsilon$ = permittivity of air, $v$ = drop velocity, $v_c$ = charge voltage, and $V_d$ = deflection voltage.

Other physical dimensions are defined in **Figure 3**. This equation gives a ±5% accuracy, which is accurate enough for our application, since the charged drops will be recycled through the ink system.

A primary consideration in the operating-point selection is to make the drop size and velocity as low as possible to minimize both the distance from the nozzle to the paper (throw length) and charge voltages. Drop size and velocity are not completely independent of each other. In order to ensure stable operation of the jet, it has been found that the kinetic energy of the jet as it emerges from the nozzle must be much greater than the potential energy associated with capillary (surface tension) forces at the nozzle exit face on the mean time the velocity of the drop has to be kept low to avoid mist generation [3].

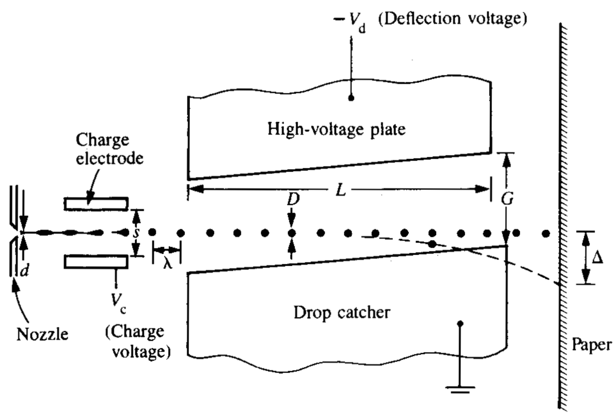


**Figure 3** Single-nozzle, binary-ink-jet schematic to define operating parameters.

For a particular drop diameter there is a band of useful velocities bounded on the bottom by directional stability criteria and at the top by misting. In practice, for jets with diameters in the 20- to 25-micrometer range, the useful velocity range is approximately 1000 to 1500 cm/s.

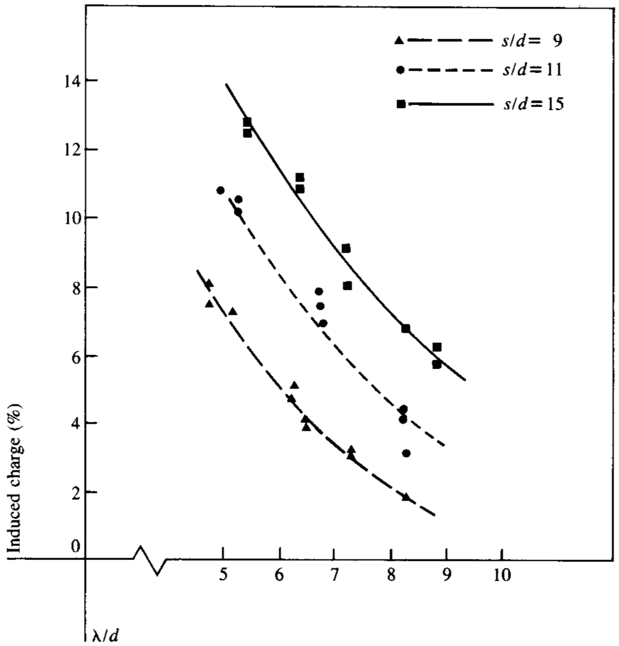


**Figure 4** Induced charge vs. $\lambda/d$ ratio with geometry as a parameter.

It is necessary at this point to consider how these operating parameters relate to the volume of ink required for image formation. Experience with an experimental water-based ink indicates that ink should be deposited at a rate equivalent to a total deposition of about 8 micrometers ink-film thickness on paper. Assume a print resolution of 240 pels per inch, corresponding to $10^{-4}$ mm$^3$ per pel. When two drops are selected per spot, the required drop volume is $5 \times 10^{-5}$ mm$^3$. The selection of a jet diameter, velocity, drop-formation rate, and separation is constrained by the well-known Rayleigh dispersion relationship [4], namely, for drop formation forced at the condition for maximum capillary growth rate,

$$\lambda = 4.5d,$$
$$D \sim 2d, \text{ and}$$
$$\lambda f = v, \tag{2}$$

where $\lambda$ is the drop separation, $d$ is the jet diameter, $D$ is the drop diameter, and $f$ is the drop formation rate.

If the jet diameter is selected as 25 micrometers and with a velocity at 1000 cm/s, the drop-generation frequency is 95 kHz. For a relative velocity between the head and paper of 250 cm/s, there are four drop-formation periods associated with each pel printed, but as stated earlier, only two drops are used. Under these conditions, a useful deflection for unwanted print drops of about 0.1 cm can be obtained with charge voltages on the order of 25 volts at a distance between the nozzle and the paper of about 1 cm.

Let us consider the consequences of the discussion thus far. By using small and slow-moving drops it is possible to achieve low-voltage operation and short throw. The correct amount of ink is delivered to the paper by using more than one drop per spot but not all of the available drops. Now consider the question of synchronization of the charge voltage relative to the drop formation. In general, if there is no synchronization there will always be an uncertainty of 1 in the number of drops that will be selected to strike the paper. This would be intolerable if the design point were precisely one drop generated per spot. For larger numbers of drops generated per spot, the deviations from average might not be significant as far as discernible print quality. On the average, the percentage of available drops per spot that is actually allowed to reach the paper will be the percentage of available time during a one-pel period in which the charge electrode voltage is off. In the asynchronous mode, it is straightforward to print while the head is slowing down and speeding up. A fixed print-pulse width is chosen to give the correct volume of ink for each pel. The print pulse is synchronized by a signal from a head-positioning sensor. If the head happens to be moving slowly, the percentage of available drops per pel actually used will be smaller, with no perceptible change in the actual printed output.

## Drop-placement accuracy

Now consider the potential sources of drop misregistration in a binary, asynchronous printer. The most obvious ones are the partial charging of a drop and differential transit time to the paper associated with pattern-dependent aerodynamic drag. The effect of partial charging of print droplets is to cause them to deviate from the trajectory of uncharged drops. The amount of deviation is given by

$$\Delta_p = \Delta Q_p/Q_T, \tag{3}$$

where $\Delta_p$ = deflection of a partially charged drop, $\Delta$ = deflection of a fully charged drop, $Q_T$ = charge carried on a fully charged drop, and $Q_p$ = charge carried on a partially charged drop.

There are three sources of partial charging. The first is an induced charge [1] which is opposite in polarity to the purposeful charge on nonprint drops. This charge depends strongly on the charge-electrode geometry and the $\lambda/d$ ratio, as indicated by the results from measurements presented in **Figure 4**. For typical parameters used in this study, the induced charge is about −7% of the charge carried on the previous drop. A second source of partial charging results from the rearward merging of a charged satellite droplet (**Figure 5**). Experiments indicate that the fractional partial charge of satellite drop is proportional to the diameter ratio of the satellite to the main drop. The proportional constant is about 0.4. Fig. 5 shows photographs of satellite formation and indicates that by choosing the wavelength-diameter ratio close to the range of maximum instability, one can ensure that the partial charge is held to less than 10%. This is to be contrasted with synchronous ink jet operation (binary or analog) where, typically, a larger wavelength is chosen along with other constraints to ensure that there are no satellites (this is the print window concept [5]). The final source of partial charging is related to the finite transition time of the voltage on the charge electrode from one state to the other. Printing experiments with and without synchronization between the drop formation and the charging process indicated that less than 5% of the printed drop was affected. The degradation in print quality was negligible.

Aerodynamic distortions of the printed pattern of a single binary-operated jet are negligible if the deflection of the guttered drop stream is small enough so that the deflected and undeflected drops travel in the same entrained air flow. However, there are significant aerodynamic problems associated with retardation of jets at each end of the array, which will be discussed below.

We now turn to some of the sources of spot misregistration that relate to the performance of an array of jets. Most generally, these result from directional, velocity, and drop-formation-distance nonuniformities along the array.

The effects of directional nonuniformity are rather straightforward, with the spot misregistration given simply by the product of the throw length and the jet directional deviation in radians. The principal defense against directional errors is to keep the throw length from the nozzle to the paper as short as possible. The situation is not quite as simple as it might seem; if the throw length is shortened by decreasing the jet velocity in order to get the necessary deflection within the shorter throw, a point is reached (as discussed above) where the jet directional accuracy is degraded. In general, above the critical velocity, the improvement in deflection sensitivity is greater than the loss in directional accuracy of the jets.

**Figure 6** illustrates the effect of velocity nonuniformity on drop registration. The drop misregistration is related to the velocity nonuniformity by

$$\textit{Spot misregistration} = v_{\mathrm{h}}\,\ell \times \textit{drop velocity variation}/v^2, \quad (4)$$

where $v_{\mathrm{h}}$ is the head velocity and $\ell$ is the distance traveled by the drop.

The sources of drop-velocity nonuniformity can be variation in the nozzle efficiency (assuming uniform pressure in the manifold behind it) or differential aerodynamic drag. In general, the edge jets tend to be aerodynamically retarded relative to the central jets. Two approaches to this problem are to have "guard" jets on the ends of the array or to create a more uniform flow by forcing air through the channel the jets travel. Variations in nozzle efficiency are to be avoided, first by selection of the physical shape (design) of the nozzle, and then by control and perfection of the fabrication process.

The jet break-off distance (BOD) nonuniformity along the array is related to the relative drop misregistration by

$$\textit{spot misregistration} = \textit{BOD nonuniformity} \times \frac{v_{\mathrm{h}}}{v}. \quad (5)$$

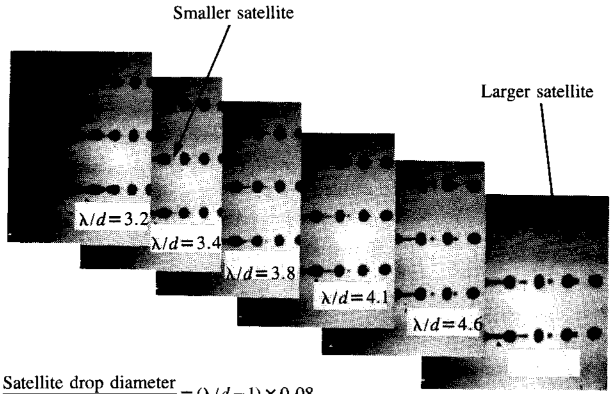


$$\frac{\text{Satellite drop diameter}}{\text{Main drop diameter}} = (\lambda/d - 1) \times 0.08$$

**Figure 5** Photomicrograph of satellite drop formation.

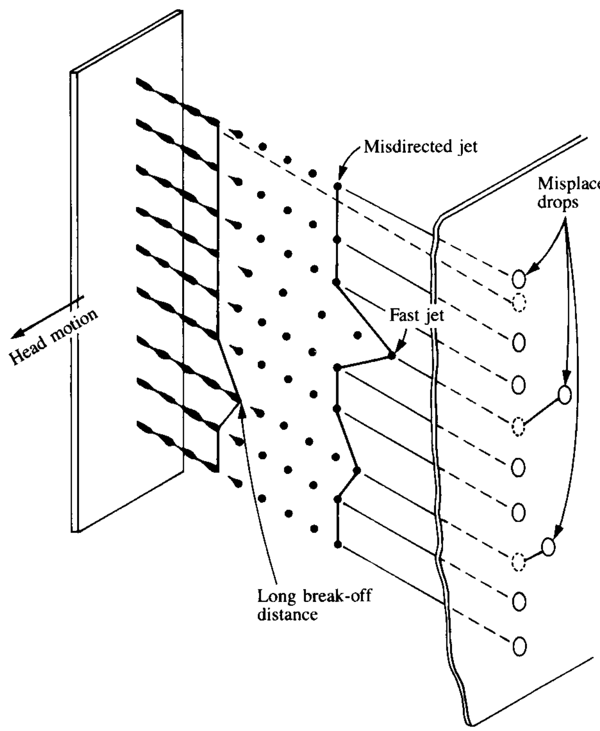


**Figure 6** Key factors affecting drop-placement accuracy.

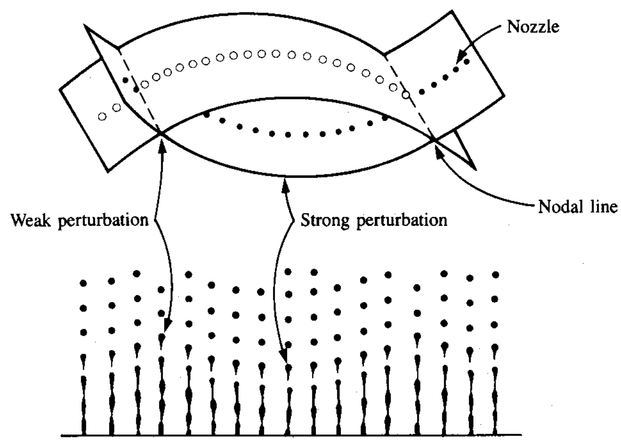


**Figure 7** Jet break-off distance uniformity vs. vibration mode shape.

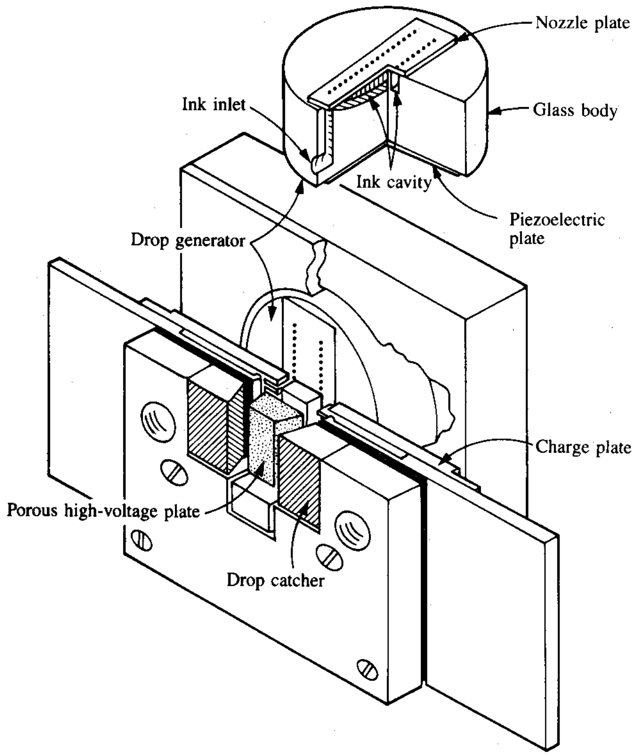


**Figure 8** Head-assembly schematic.

The primary source of the BOD variation is the nonuniform vibrational perturbation on the nozzle plate along the array. This is avoided by designing the head so that no nodal line cuts across the jet array at the drop-generating frequency (**Figure 7**).

Our experience with two 25.4-mm (1-in.)-long arrays of 240 nozzles is that directional uniformity < ±3 milliradians, velocity uniformity < ±1%, and jet BOD variation < ±0.1 mm give a root mean square value of the drop-registration error of ±0.05 mm for the operating point described above.

## Head design, fabrication, and performance

• *Drop generator*

The nozzle array is etched into a silicon chip that is bonded to a glass block containing the ink manifolds. A thin piezoelectric ceramic disk bonded to the opposite face of the glass block provides the mechanical perturbation required for uniform periodic drop formation of the jets. An input filter serves to guard against clogging. The drop generator is shown in **Figure 8** [6].

The nozzles are holes with the shape of a truncated pyramid etched into a silicon substrate [7, 8]. **Figure 9** shows a scanning electron micrograph of both an individual nozzle and a segment of an array. The shape of the hole is determined by the anisotropic characteristics of the silicon etch. By using thin silicon substrates it is possible to place the nozzles on 0.2032-mm (0.0083-in.) centers as required for a two-row 240-pel-per-inch print head.

The unusual shape of the holes has some important fluid dynamic consequences. As might be expected, the convergent shape of the nozzles makes them very efficient (low-pressure drop) and insensitive to area variations. Figure 9 shows the velocity sensitivity factor with respect to the nozzle size as a function of ink viscosity and nozzle size. In order to maintain velocity uniformity of ±1% it is necessary to control the orifice area to ±6% for an ink with viscosity of 2 c.s. ($2 \times 10^{-6}$ $m^2/s$). This corresponds to a linear photolithographic tolerance of ±0.6 micrometer, a stringent requirement. Another property of this nozzle geometry is the difficulty of achieving satellite-free operation. Hence our nominal print condition was with rear-merged satellites, as shown in Fig. 5. This may be a consequence of both the high efficiency and the square shape. The jet relaxes from the square shape at the nozzle exit to the cylinder in a time that is short compared to drop-formation time [9].

The glass block is carefully designed to ensure that over a band of frequencies centered on the operating frequency the piezoelectric driver will cause a uniform displacement of the entire nozzle array. The resulting velocity perturbation causes capillary instability of the jet and controls the rate of drop formation. It is to be contrasted with the complementary approach of pressure perturbation [10]. Although drop-formation-length uniformity is not of fundamental importance in asynchronous printing, good results have been achieved (**Figure 10**).

• *Charge electrode*

The charge electrode array is composed of slots formed in the edge of a ceramic plate. The slots are metallized and isolated from each other and connected to a cable by printed-circuit conductive lines on the flat surface of the plate. A plate is bonded over the flat surface to passivate it against electrochemical corrosion. **Figure 11** is a schematic of the electrode array. Two such pieces face each other, as indicated in Fig. 8, each with slots on 0.213-mm centers and displaced from each other along the array axis by 0.106 mm.

• *Deflection and guttering*

The deflection and guttering structure is shown schematically in Fig. 8. A high-voltage plate is positioned between the two linear arrays of jets, which are deflected in opposite directions into porous catchers that serve as the ground electrodes. Careful attention must be paid to the selection of the porous material and the design of the manifold behind the material to ensure that there is no excessive air flow due to the vacuum applied to the drop catchers. The goal of the design has been to have fluid to block transverse air flow that could degrade the image. Another consideration in the design was to minimize misting from drop impacts. The key factor in that respect is to optimize the angle of impact. Experiments indicate that if the normal component of the drop velocity is too small, the drop can be bounced off the porous surface like a ping-pong ball. On the other hand, mist will be generated if the normal component becomes too large. The optimum impact angle we selected for our system was 9°.

• *Start-up and maintenance*

The head components are assembled with gaskets, ducts, and channels to facilitate a novel start-up and cleaning approach, which was part of the study. The assembly is schematized in **Figure 12**. During start-up the head is positioned at a maintenance station located along the head-transport mechanism beyond the edge of the paper path. The head is completely flooded with ink supplied by the nozzles. When the head cavities are full, a vacuum is applied to the main channel opening (where the jets emerge) and air is allowed to flow through the ducts to clear fluid from the charge-electrode constrictions. Typically, it takes about one minute for an electrically nominal "dry" condition to be reached. Periodically, the head is returned to the maintenance station to be flushed clear of any paper fibers or other debris that may have accumulated.

• *Materials considerations*

The drop generator contains some of the most significant challenges from a materials-technology viewpoint. All of the materials in contact with the ink must be carefully selected so as to be compatible with the ink and with one another. The entire assembly, including the filter, must be very carefully assembled under controlled conditions to ensure that there are no contaminants in the head capable of migrating to the orifices. The conductors in the charge-electrode slots must be uncoated to achieve correct electrical operation (no surface

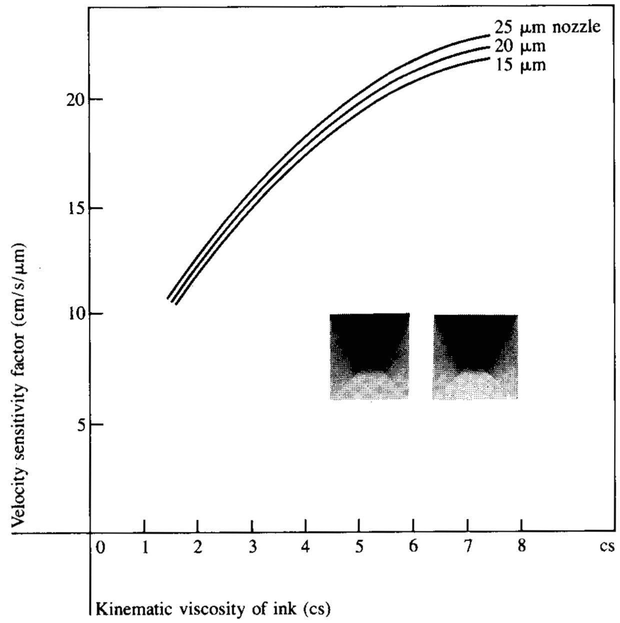


**Figure 9** Jet velocity sensitivity for silicon nozzle and scanning electron micrograph.

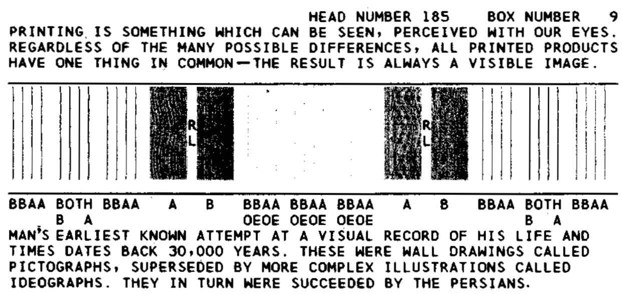


**Figure 10** Print sample from 25.4-mm (1-in.) head printing experiment.

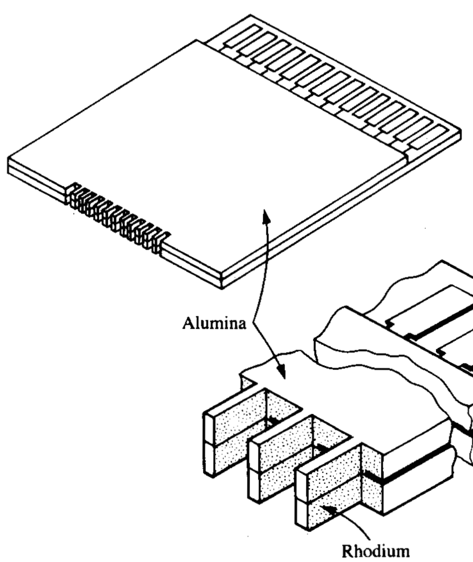


**Figure 11** Schematic of charge electrode array.

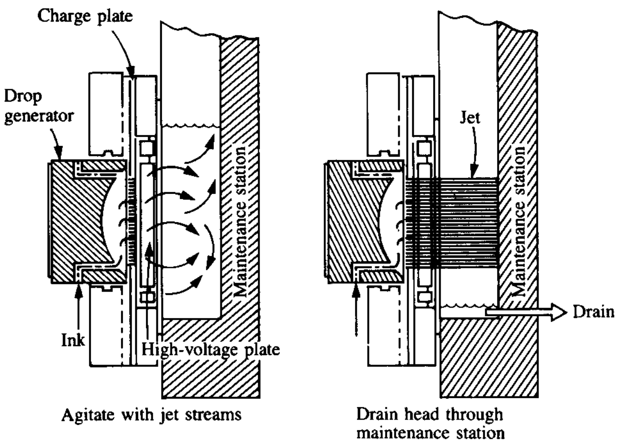


**Figure 12** Head assembly with start-up fluid and air flows indicated.

charge build-up). They are operated under conditions which create susceptibility to electrochemical corrosion. Materials selection and processing and head-operating conditions must be carefully selected to minimize this problem.

• *Printing experiments*

Printing experiments were carried out on a prototype device. The head was transported across a 36-cm-wide fanfold paper path printing a 25.4-mm (1-in.) swath. The peak transport velocity was 250 cm/s. The paper was moved in precise 25.4-mm (1-in.) increments during the 50-ms period of turnaround and no printing. The print sample is reproduced in Fig. 10. The background is very clean and the overall print quality is acceptable for many system-printer applications.

## Discussion

Some of the highlights of the asynchronous, multiple-drop-per-spot mode are 1) no print window, 2) variable-speed printing, 3) no phase between drop formation and print signal, 4) no aerodynamic or charge interaction corrections, and 5) no mist generation. The fabrication techniques described are essentially batch techniques, which are sensitive in cost more as it relates to the size of the head than to the number of jets, and thus very well suited to the operating point. The approach is modular and can be applied to a variety of printer configurations.

Areas that have shown positive evaluation results but need significant further work in order to ensure a successful high-reliability product are 1) sensitivity of the head to paper-fiber (dust) contamination, 2) wet start-up reliability, and 3) electrochemical corrosion on the charge-electrode array.

## Acknowledgments

The authors wish to acknowledge the many contributions of their co-workers at the IBM Thomas J. Watson Research Center in Yorktown and the IBM General Products Division Laboratory in San Jose. The contributions of Erik Solyst, in particular, are gratefully appreciated.

## References

1. G. L. Fillmore, W. L. Buehner, and D. L. West, "Deflection in an Electrostatic Ink Jet Printer," *IBM J. Res. Develop.* **21,** 37–47 (1977).
2. Dijit Systems Brochure, Mead Corporation, Dayton, OH, 1973.
3. J. L. Zable, "Splatter During Ink Jet Printing," *IBM J. Res. Develop.* **21,** 315–320 (1977).
4. J. W. S. Rayleigh, "On the Instability of Jets," *Proc. Lond. Math. Soc.* **10,** 4 (1878).
5. S. A. Curry and H. Portig, "Scale Model of an Ink Jet," *IBM J. Res. Develop.* **21,** 10–20 (1977).
6. F. P. Giordanno, L. Kuhn, R. Lane, C. H. Lee, and G. Zierdt, "Ink Jet Printing Head," U.S. Patent 4,188,635, February 1980.
7. E. Bassous, H. H. Taub, and L. Kuhn, "Ink Jet Printing Nozzle Arrays Etched in Silicon," *Appl. Phys. Lett.* **31,** 135 (1977).
8. R. H. Kurth, "Process for Producing Uniform Nozzle Orifice in Silicon Wafers," U.S. Patent 4,169,008, September 1979.
9. M. Levanoni, "Study of Fluid Flow through Scaled-up Ink Jet Nozzles," *IBM J. Res. Develop.* **21,** 56–68 (1977).
10. G. L. Fillmore and D. C. Van Lokeren, "A Multinozzle Drop Generator Which Produces Uniform Breakup of Continuous Jets," *IEEE-IAS Conference Proceedings*, October 4–8, 1982.

*Received October 10, 1983; revised November 30, 1983*

**Richard H. Darling** *IBM General Products Division, Tucson, Arizona 85744.* Mr. Darling is a program manager in the Tucson laboratory working on the development of a new non-impact printer. He joined IBM in San Jose, California, in 1959, working in the unit records area. In 1965 he received his B.S. in electrical engineering at San Jose State University, California. Through his career he has worked in San Jose, Boca Raton, Florida, Endicott, New York, and Tucson. His development activities cover unit record card I/O, magnetic card systems, disk and tape drives, and extensive impact and non-impact printer efforts. Mr. Darling has received two IBM Outstanding Contribution Awards, a First Level Invention Achievement Award, and a Corporate Outstanding Invention Award.

**Lawrence Kuhn** *Decision Data Computer Corporation, 100 Witmer Road, Horsham, Pennsylvania 19044.* Dr. Kuhn is currently project manager for the Decision Data Computer Corporation, which he joined in August 1983. Prior to that, he was a senior engineer with the IBM General Products Division in both San Jose, California, and Tucson, Arizona, from 1978 to 1983, and a Research staff member at the IBM Thomas J. Watson Research Center, Yorktown Heights, New York, from 1968 to 1978. He received a B.S. in 1964, an M.S. in 1965, and an Eng.Sc.D. in 1968 from Columbia University, New York. His technical activities have been primarily in the areas of non-impact printing, laser machining, integrated optics, surface acoustic waves, and plasma physics.

**Chen-Hsiung (Bernard) Lee** *IBM General Products Division, 5600 Cottle Road, San Jose, California 95193.* Dr. Lee is a senior engineer in the General Products Division laboratory at San Jose. He joined IBM in 1968 at Endicott, New York. From 1968 to 1972, he worked on mechanics and thermal problems associated with packaging and impact printers, moving to San Jose in 1973 to work on non-impact printers. He is currently involved with robotics and advanced file product development. Dr. Lee received his Ph.D. in theoretical and applied mechanics from Cornell University, Ithaca, New York.